Benchmarking of potential substituents for leaded bronze in axial sliding bearings for mobile hydraulic applications

Galina Haidarschin*, Mareike Hesebeck*, Eddy Su* and Marc Diesselberg*

*Danfoss Power Solutions, Krokamp 35, D-24537 Neumünster, Germany
E-Mail: ghaidarschin@danfoss.com

This study comprises testing of RoHS-compliant axial sliding bearing materials, including bronzes, brasses, thermally sprayed coatings and PVD coatings, in a pin-on-disc tribometer and bench testing in an axial piston pump. The aim was to compare and benchmark these materials against commonly utilized leaded bronze with respect to durability and tribological mechanisms and to derive principles for axial sliding bearing material suitability in hydrostatic components. By evaluating the test results, some fundamental understanding was gained about characteristics which materials must exhibit to achieve sufficient tribological performance and durability in hydrostatic components including, but not limited to resistance against friction-induced material transformation and sufficient ductility to withstand pressure-induced part deflection.

Keywords: Axial piston pumps and motors, axial sliding bearing materials, RoHS-compliance, tribology
Target audience: Mobile Hydraulics, Machine Manufacturers, Bearing Material Suppliers

1 Introduction

Leaded bronze has been a long-established material applied in axial sliding bearings for hydraulic applications due to its outstanding performance under starved, mixed, and fully lubricated conditions. However, among other things, environmental restrictions described for example in EU directive 2011-65-EU (*Restriction of Hazardous Substances Directive* aka. RoHS2) drive the substitution of leaded bronze by novel materials in certain applications. For automotive applications, alternative materials like non-leaded bronzes and brasses, thermally sprayed coatings and physical-vapour deposited thin films have been already successfully implemented. Nonetheless, for hydrostatic components, a potential substitute with equal or better wear protection like leaded-bronze is still being pursued. The aim of this study was to compare and benchmark these materials against commonly used leaded bronze with respect to durability and tribological mechanisms and to derive principles for axial sliding bearing material suitability in hydrostatic components.

2 State of the art

In a hydrostatic axial piston pump, in particular a swashplate type, there are several interfaces that are tribologically loaded during operation, i.e. several parts are sliding and/or rolling against a counterpart while being fully or partially separated by a (usually fully formulated) hydraulic fluid. For those interfaces, which might see severe metal-to-metal contact during operation, sufficient wear resistance of the material is needed for both normal operating conditions like break-in as well as in abnormal conditions, i.e. intermediate local fluid film breakdown because of fluid foaming or else. One of these bearing interfaces is the pair comprising the rotating piston-containing cylinder block and the valve plate (sometimes called differently depending on component design and manufacturer). As the (slightly tilted) block is rotating with rotational velocity of up to several thousands of rpm, corresponding to a speed of up to 40 m/s, and as an intermediate fluid film breakdown can happen in certain conditions, the valve plate material must withstand very high metal-to-metal sudden impact energies without losing its bearing function for the rest of the component's lifetime.

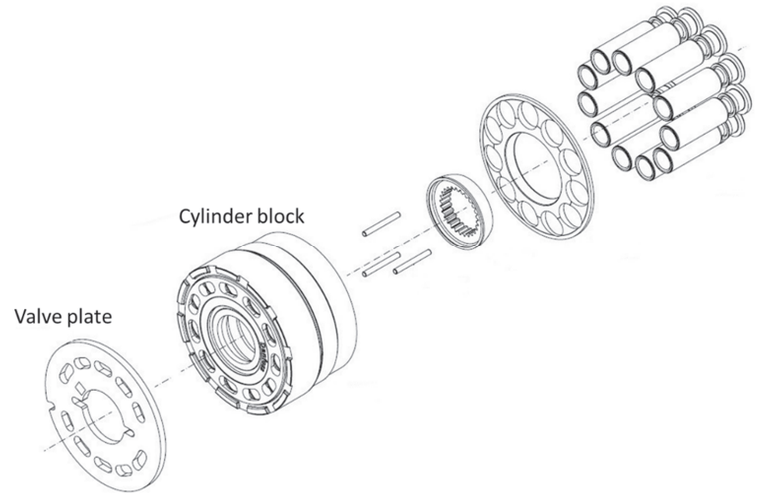

Figure 1: Exploded view of the rotational kit of a swashplate type axial piston pump

A material that has been successfully used for decades to fulfil this emergency bearing function is leaded bronze, sometimes as bulk material, often as thick layer on a steel part. The copper in that alloy exhibits good oxidation resistance, sufficient strength and ductility. The function of lead itself in bronze is not fully understood in detail, but several hypotheses have been published. The solid insolubility of lead within a copper microstructure, leads to segregations of large lead particles along the grain boundaries. /1/ Due to the low melting point of lead of 327.5°C, near-surface particles will melt under frictional heating and smear across both tribological partners, thus separating the solid metal parts from each other and preventing fatigue wear. /2/ At the same time, the near-surface removal of lead leaves voids which can act as supplemental fluid reservoirs in addition to the existing valleys of the original surface finish. Despite the excellent tribological properties as axial sliding bearing material in axial piston pumps, lead exhibits some disadvantages of which especially the environmentally hazardous properties have gained significant attention in the recent past, as mentioned in the introduction.

For many years, alternative materials have become commonly available and are being successfully utilized, for example, by the automotive industry. However, these materials have not reached full market penetration in the mobile hydraulic machinery yet. As an example, amorphous carbon coatings commonly known as diamond-like-carbon (DLC) are widely used in industry as coating for tappets, piston pins, and in diesel injection systems. /3/ However, DLC films have shown issues when applied on hydrostatic components. Besides common and potentially resolvable technical problems such as ductility to withstand the pressure-induced part deflection or substrate bonding issues, other obstacles including the insufficient heat transfer capability, the low thermal stability up to 300°C /4/ and the resulting heat-induced graphitization with accompanying low wear resistance, have principally prevented a successful application in hydrostatic components thus far.

Further examples of substitutes for leaded bronze are lead-free bronzes and brasses. Several groups are investigating the performance of different lead-free bronzes in comparison with leaded bronze, showing e.g. for CuSn12Ni2 a lower wear level /5/ or a strong speed/pressure dependency on the performance of aluminium bronze. /6/ However, previous tests (not published) did also show that some of these materials did not achieve similar performance levels while tested in hydrostatic components. To improve the performance level of lead-free copper alloys and to mimic the beneficial effect of lead described above, several groups have published experiments with bismuth containing bronze. /7/ On a laboratory scale, some promising results were achieved, however no experience is currently available with applications in actual hydrostatic components or even field use.

Other lead-free materials such as polymers or composite materials have several issues with the thermal stability as well. Polyetheretherketone (PEEK) is a high-performance polymer with excellent mechanical, chemical and

thermal properties. Additionally, this material exhibits low coefficient of friction and low wear rate in comparison to other polymers. Its properties allow an application in journal bearings and piston rings. However, its low glass transition temperature of 143-162°C and melting temperature between 343-387°C are limiting factors for its application as a valve plate component. /8/

Another wear resistant material system that is being utilized successfully in automotive applications are thermally sprayed coatings based on iron and molybdenum. This coating system is used in internal combustion engines as liner materials that carries piston and piston ring loads./9/ It has not been tested as an axial sliding bearing material thus far.

3 Experimental details

3.1 Materials

10 different materials from three different classes have been chosen (ref. Table 1) for the purpose of comparison with the leaded bronze.

Class	Designation	Material type	Processing type	Hardness	Layer thickness	Carrier material
Cu-based	CuSnPb	Leaded bronze	Sintering on steel strip	106.0 ± 4.0 HBW 1/5/30	358 ± 8 µm	C22
Cu-based	CuNiSi	Copper alloy	Casting on steel strip	117.0 ± 2.5 HBW 1/5/30	1032 ± 4 µm	C22
Cu-based	CuSn	Tin bronze	Sintering on steel strip	78.9 ± 1.3 HBW 1/5/30	540 ± 5 µm	C22 or similar
Cu-based	CuSnBi	Bismuth bronze	Sintering on steel strip	75.7 ± 2.6 HBW 1/5/30	504 ± 7 µm	C22 or similar
Cu-based	CuZn	Brass	Ingot casting	92.1 ± 0.5 HRB	-	-
Cu-based	CuZn+MoS_2	Brass with coating	Ingot casting + cold spraying	92.1 ± 0.5 HRB (CuZn)	8 µm	CuZn
Thermal Spray	Fe-base	Thermally sprayed coating	Atmospheric plasma spray on steel substrate	436 ± 22 HV0.3	131 ± 7 µm	C22
Thermal Spray	Mo-base	Thermally sprayed coating	Atmospheric plasma spray on steel substrate	573 ± 43 HV0.3	102 ± 5 µm	C22
PVD coating	Cr-base	Nitride multilayer	Cathodic arc deposition on steel substrate	19GPa	5.4 µm	42CrMo4 HH+QT
PVD coating	Ni-base	Metal layer	Cathodic arc deposition on steel substrate	7 GPa	5.9 µm	42CrMo4 HH+QT
PVD coating	Al-base	Oxide layer	Cathodic arc deposition on steel substrate.	25 GPa	4.6 µm	42CrMo4 HH+QT

Table 1: Overview of tested valve plate materials

Based on the investigated material, different carrier materials are selected, depending on the requirements of each bearing material. The influence of the backing material on the performance of the material is not part of this study. The roughness of the tested hardware is adjusted to the current standards in the automotive and bearing application and thus is not comparable among the samples. The same is valid for physical properties, such as the hardness of the coating.

The counterpart for the valve plate is a cylinder block, manufactured out of powder metal material, infiltrated with copper. Some of the parameters of the steel surface are listed in Table 2.

Hardness	Rpk [µm]	Rk [µm]	Rvk [µm]
89 HRB	1.3	0.65	0.55

Table 2: Parameters of the cylinder block

3.2 Testing procedure

According to DIN 50322, every test can be categorized into one of six classes, depending on their complexity. Field-testing in real machines as the test with the highest comparability to the real application is considered as category one. On the other end of the scale (category six), tribometer tests show the lowest comparability as simplified special parts and test conditions are used. These tests are conducted to understand the material properties in loaded conditions and to become a first indication of the performance in real application by comparing with the known material. The test stand is located between the field-testing and the tribometer testing in category three. With this test, real components under laboratory conditions on a test stand are tested.

For this study, pin-on-disc tribometer tests and full-sized Danfoss pump tests are used for benchmarking the alternative materials against the standard leaded-bronze.

3.2.1 Tribometer tests

For the comparison of the materials properties such as abrasive and adhesive wear resistance, a pin-on-disc tribometer setup with a UMT-3 tribometer (Bruker) is taken. The tested material is applied on discs. The surface parameters of the tested materials are listed in Table 3.

Material	Rpk [µm]	Rk [µm]	Rvk [µm]
CuSnPb	0.55 ± 0.1	1.18 ± 0.05	0.69 ± 0.06
CuNiSi	0.56 ± 0.08	1.10 ±0.03	0.62 ± 0.06
CuSn	0.45 ± 0.03	0.96 ± 0.02	0.51 ± 0.03
CuSnBi	0.42 ± 0.06	0.95 ± 0.07	0.60 ± 0.07
CuZn	0.16 ± 0.04	0.7 ± 0.1	0.5 ± 0.2
CuZn+MoS_2	21 ± 3	18 ± 5	2.8 ± 0.5
Fe-base	0.008 ± 0.001	0.028 ± 0.001	0.8 ± 0.1
Mo-base	0.008 ± 0.001	0.026 ± 0.001	0.8 ± 0.3
Pin	2 ± 1	3 ± 1	2 ± 2

Table 3: Surface roughness of the tested tribometer samples

For the counterpart, pins manufactured from powder metal material, similar to the material of the cylinder blocks are manufactured. To ensure that no rapid contact area changes due to a tilting of the pin are possible, and to increase the contact pressure by reducing the contact area, a half-sphere shape with a diameter of 10 mm is fine-turned at the test end of the pin. Lubricated conditions during the test are realized by a splash lubrication with a non-additivated group II mineral oil based hydraulic fluid VG 46. Using the base oil excludes the impact of the additives, which might influence the performance of various material classes differently. To analyse the steady-state behaviour of a tested material, a long-term test under a steady load is carried out. The test conditions are shown in Figure 2.

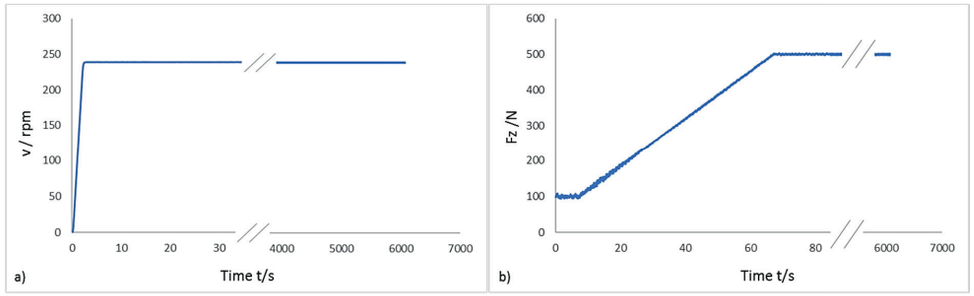

Figure 2: Test conditions of the tribometer steady state test

After a 10 s running-in period at a load of 100N, the load is increased to 500 N within 60 s and then held for 6000 s at a circumferential speed of about 0.5 m/s. The rotational speed is chosen to ensure mixed lubrication conditions during the test. The tests starts at ambient temperature (22±1°C). The temperature is neither controlled nor tracked during the tests.

One of the main results from the tribometer testing are the *Coefficient of Friction* (COF) curves. The COF of a system depends on many parameters, such as surface roughness, hardness of contact partners, chemical bonding, etc. The behavior of the COF curve during the test indicates the performance of the material and the stability of the chosen pairing. A high coefficient of friction in a real component causes decreased efficiency and additionally, increase of frictional heat, which consequently results in shrinkage of the fluid film separating the surfaces, subsequent breakdown of lubrication and at the end, damage of components.

3.2.2 Component testing procedure

For component testing, axial piston pump was utilized and operated with the same conditions at the same test bench for each material. In every test run, the complete rotating kit, including the stationary valve plate, copper-infiltrated steel cylinder block and the pistons, were replaced to avoid influences from previous test runs (e.g. break-in, contamination). The test sequence consisted of ten consecutive steps of pressure and speed increase, finally exceeding rated values by approximately 20%. During the test, several parameters were observed to be able to stop the test in case of detected irregularities. The component testing sequence was considered as successfully passed, if all steps of pressure and speed increase had been executed without any occurrence of abnormal pressure drop or case-flow increase during the overall testing time of 90 min, which would indicate leakage between valve plate and cylinder block due to wear. For statistical analysis of the results, three tests for each material were performed. For the comparison of the results, PV-factors for different materials achieved during the test were calculated. Therefore, for materials with strong variation of the test results, the minimum achieved value is selected. The PV factor represents the product of the pressure P (case pressure during the test) with the sliding velocity V (rotational speed of the kit) of the latest successfully passed testing stage and gives information regarding the contact lubrication severity. /10/

3.3 Wear characterization

For evaluation of the wear volume on the tribometer samples, 2D and 3D profilometry is used for the discs and pins, respectively. Thereby measurements with a tactile profilometer are taken perpendicular to the wear track using a Zeiss Surfcom 5000. For the calculation of the total wear volume over the disc, the wear area, determined on the 2D wear profile, shown in red in Figure 3, is multiplied with the total length of the wear track (eq. 1).

$$V_w = 2\pi R \cdot A \quad (1)$$

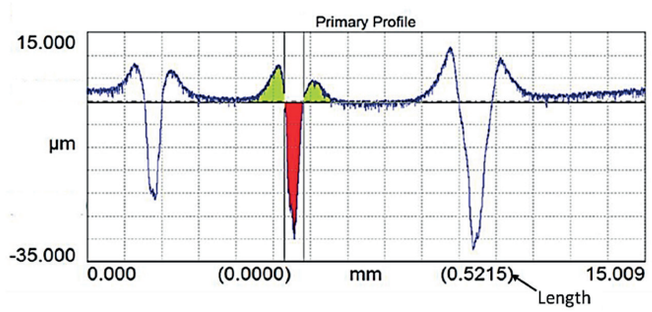

Figure 3: Wear area measurement

For statistical evaluation, the wear area is measured on three different positions of the wear track. For calculation of the wear volume, which is defined as the total material loss, the material accumulations at the edges of the wear track need to be subtracted from the calculated value (see green areas in Figure 3). For the pins, the wear volume was calculated using the confocal microscope Neox-S of Sensofar and by using the software SensoMaps. Therefore, the measured wear area at the tip of the pin is converted into a cavity and the volume of it is calculated (see Figure 4).

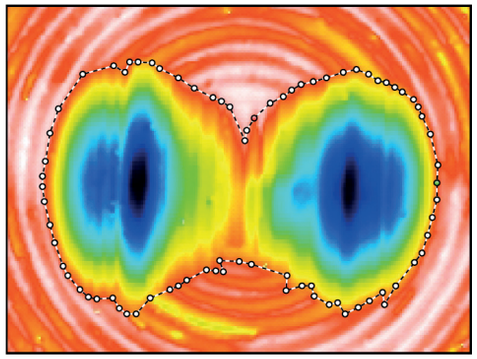

Figure 4: 3D wear volume measurement on the pin

Regarding the tribological analysis of the component hardware, both valve plate and cylinder block were analysed using a Zeiss-made Scanning Electron Microscope (SEM) with Oxford-brand Energy Dispersive X-ray detector. Deep dive analysis of the microstructure is carried out by using the Leica DMi 8 A optical microscope.

4 Results and Discussion

4.1 Tribometer test

One key response from the tribometer testing was the coefficient of friction (COF) during the constant load test. The summary of all curves is shown in Figure 5. The pin-on-disc test has shown significant principal differences in the progression of the COF of above mentioned materials.

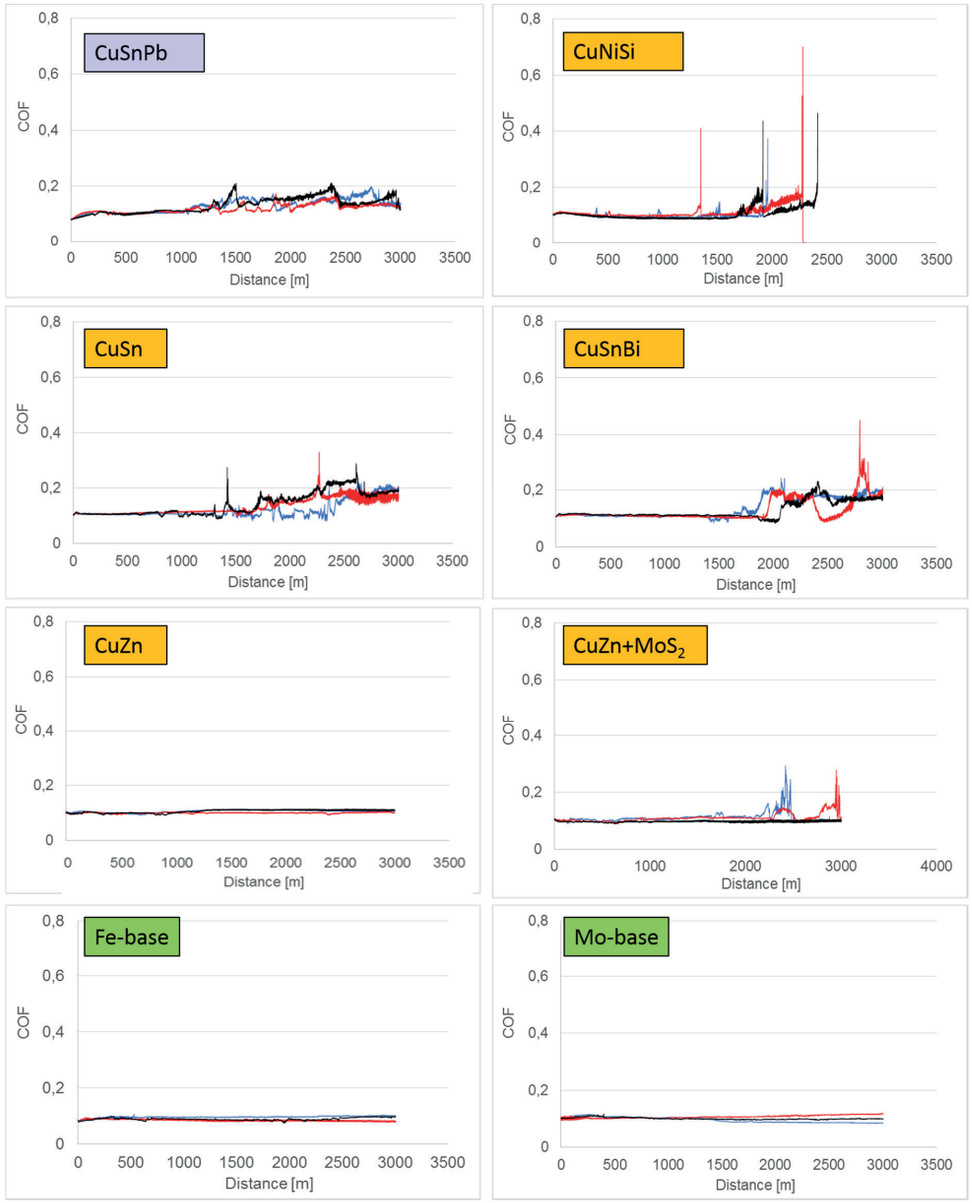

Figure 5: Coefficient of friction curves for different materials

The reference CuSnPb shows a continuous increase of the COF up to 0.2 and some fluctuations of the curve. CuNiSi material, in contrast, shows very stable COF progressions until a sudden increase to over 0.5 occurs, which triggered a stop of the test, indicating adhesive wear and tribological failure. CuSn and CuSnBi have comparable behaviour as the leaded bronze with slightly higher increase of the COF up to 0.3 during the test. The fluctuations of the curve, which can be seen as a sudden increase of the COF with immediate decrease are interpreted as a result of temporary welding of the two contact partners or temporary accumulation of larger amounts of wear debris in front of the pin. CuZn and CuZn+MoS_2 show different results respectively. While the CuZn samples have a stable behaviour throughout the test with a constant COF of 0.1, the CuZn+MoS_2 samples show a strong increase of COF at the end of the test but without exceeding a value of 0.3, which is likely attributed to larger amounts of wear debris of the topmost MoS_2 coating. Thermal sprays of Fe-base and Mo-base show, in addition to uncoated brass, demonstrated the most stable behaviour of the COF in comparison with other tested materials, reaching a maximum value of 0.1 and 0.12 respectively, indicating only a very slight change in material or surface properties. In case of the PVD coatings, the test had to be halted after only a few seconds due to premature coating failure, which is related to the initially contact pressures applied during this test. Therefore, these coatings needed to be excluded from evaluation.

The respective calculated wear volumes for the discs and the pin are shown in Figure 6. The reference bronze shows the highest average wear of the pin of 0.27 mm^3, compared to other tested materials. The calculated value for the average wear on the disc amounts to 1.31 mm^3. Other copper-based materials, besides the manganese silicide fortified brass materials, show similar wear volumes as the reference. It must be noted that the calculated wear volume of CuNiBi is not comparable with the other samples, since the tests were prematurely stopped and are marked red for this reason. CuZn and CuZn+MoS_2 show different wear volumes, of which CuZn shows a lower materials loss compared to the reference. Even if the composite hardness of CuZn was measured to be lower than that of the leaded bronze, the embedded (hard) manganese silicide particles, which are oriented parallel to the running surface, significantly improve the wear resistance. CuZn+MoS_2, including soft carbon-based coating at the top apparently shows the highest material removal on the surface. However, this result is misleading because it includes material removal of the sacrificial MoS_2 layer, which is intended. This soft layer is easily removed by abrasive wear due to the locally applied initial high contact pressure by the pin. The two thermal sprays (Fe-base and Mo-base) resulted in the lowest material loss in this study as well as for the disc (0.43 mm^3 and 0.35 mm^3) as for the pin (0.01 mm^3 and 0.03 mm^3). This is mainly related to relatively high hardness, resulting in high abrasive wear resistance (Archard's law), smoother surfaces, causing less material removal during break-in and manufacturing-process-related high density of pores in the surface, which act as fluid reservoirs thus improving the lubrication.

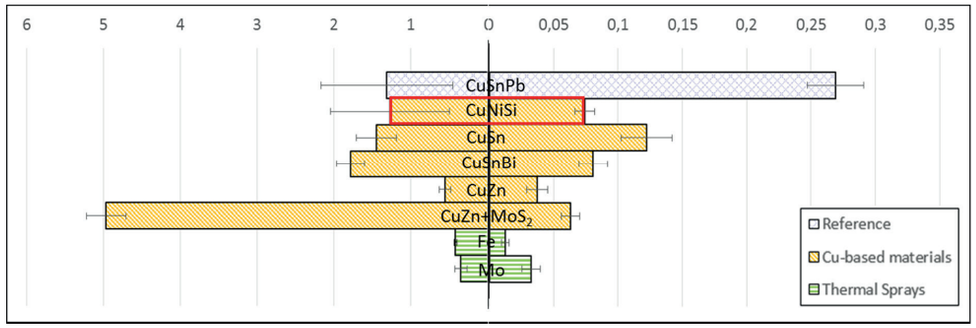

Figure 6: Wear volumes after the constant load test for Disc (left) and the Pin (right, different scale)

4.2 Component test

As described in the experimental details, all materials were benchmarked against the leaded bronze by calculating the PV factor of the last sequence step prior to test abort, if occurred. The bi-metal leaded bronze reference valve plate was one of the materials that successfully passed the sequence, therefore achieving the highest possible PV factor in the last step of this test sequence. The normalized PV factors for all tested materials are shown in Figure 7.

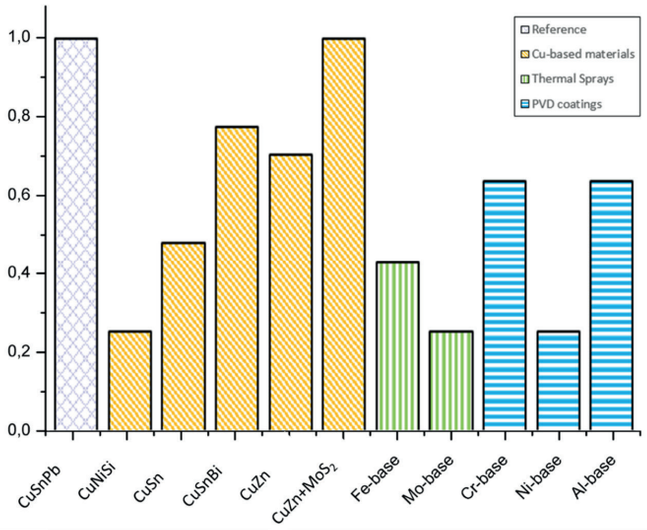

Figure 7: PV factors reached before test stop/abort (normalized)

All copper-base materials, highlighted in orange, are showing large variation in achieved PV factors, ranging from 25 to 100% of the reference bronze, i.e. only one material (brass+MoS_2) besides leaded bronze ran though the complete testing sequence without test abort. Both thermal sprays, shown in green, remain below 43%, while the PVD coatings, highlighted blue, range from 25 to 64%. To interpret this high variation of results, which is not meeting the performance expectations based on successful usage in automotive and other bearing applications, a detailed analysis of the wear tracks on the valve plate and the cylinder block was performed.

Therefore, scanning electron images of the plates' raceways are shown in Figure 8. The reference bronze CuSnPb shows only mild polishing with removal of some surface peaks. The valleys of the initial surface finish are still present. No other major wear mechanisms beside minor abrasive wear (scratches) were detected.

For all other copper-based material, except the MoS_2-coated version, strong deformation, material transfer, chunk formation and signs of fatigue were detected. For non-coated CuZn brass and CuNiSi, clear indications of adhesive wear were observed. In these cases, the original surface was no longer even partly visible. The cross-sectional microstructure analysis of these parts (Figure 10) shows a material transformation below the raceway, resulting in finer grains. In the case of CuSn and CuSnBi, this transformation leads to embrittlement of the microstructure, formation of microcracks and subsequent delamination of the transformed sublayer. Alloying with bismuth, which arranges along the grain boundaries is said to weaken those and enhances the forming of microcracks additionally. /11/

This detrimental friction-induced material transformation happens in metal-to-metal contact situations, because the (naturally slightly tilted) rotating cylinder block locally touches the (naturally slightly deflected) valve plate with speed of several thousand rpm (up to 40 m/s) and high resulting contact energy that converts very locally into friction, heat and/or material deformation. This detrimental effect has been earlier identified for amorphous carbon coatings (DLC) as well which transform to graphite under frictional heating within seconds.

The addition of MoS_2 coating to the brass material surface results in a significant improvement of the performance over the non-coated brass, also seen in the achieved PV factor. The raceway shows only a slight decrease of the film thickness in areas of the highest contact.

For the Fe-based thermal spray, the appearance of the affected surface does not indicate any enhanced wear. Only a mild polishing of the surface can be observed, which is corresponding to the results from tribometer testing. However, on a macroscopic scale, this coating exhibited a significant issue with the coating bond to the substrate at the edges of the kidneys in the high-pressure area of the valve plate, leading to partial coating delamination (not shown) finally resulting in a significant change in hydrodynamic/hydrostatic balance and leakage.

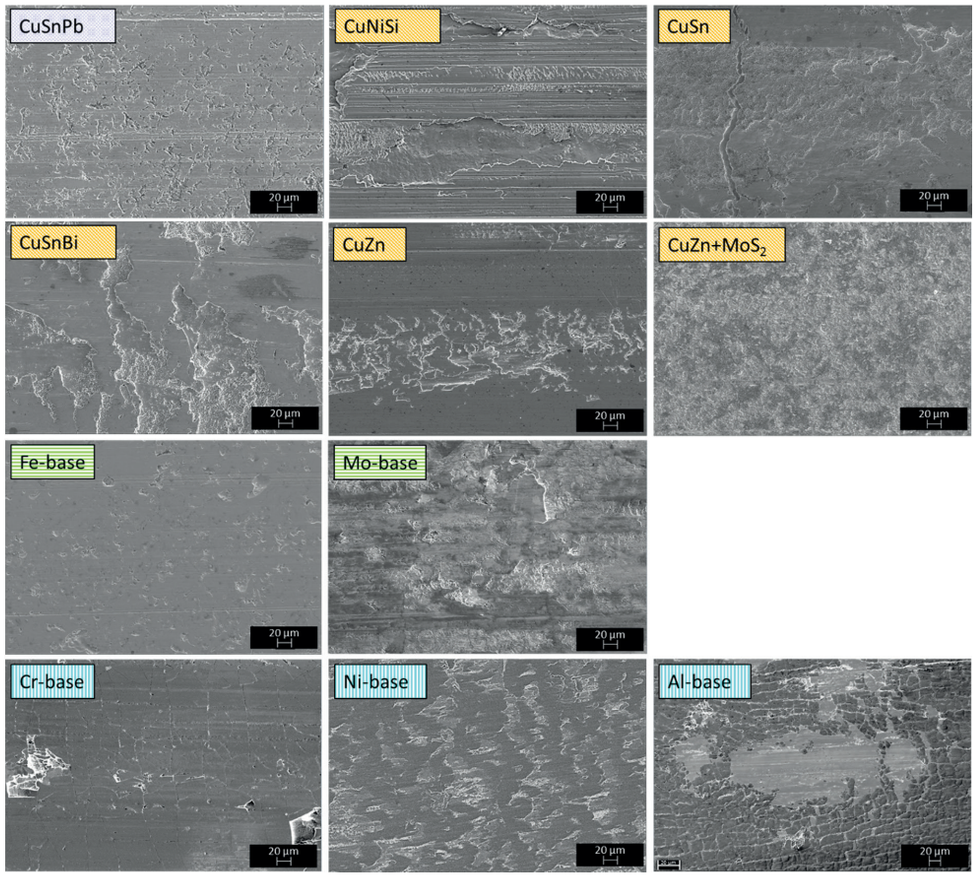

Figure 8: SEM images of the wear tracks

Concerning the Mo-based thermal spray, adhesive wear can be detected in the wear track. Additionally, delamination in the edge areas of the kidneys (shown in Figure 9) is observed for this coating as well.

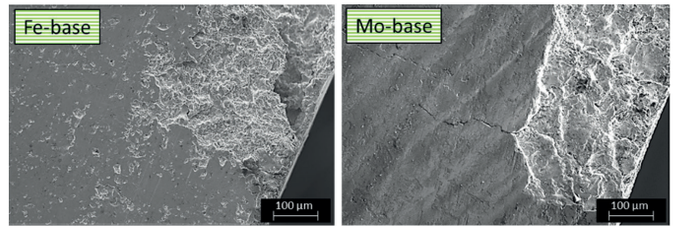

Figure 9: Delamination in the edges of the kidneys for thermal sprays

The investigated three PVD coatings are showing different wear mechanisms in this application.

In the case of the Cr-based nitride PVD coating, cracks were observed all over the raceway. This is in relation to shear stresses caused by a high coefficient of friction exceeding the coatings ductility. In addition, the relatively low temperature resistance of this coating (300°C), which is exceeded in certain spots of the surface, will likely lead to a detrimental change of coating intrinsic properties.

For the Ni-based PVD coating, a strong adhesion tendency to the counterpart has been detected, leading to massive material transfer, surface roughening (formation of scales) and wear of the counterpart.

The Al-based oxide PVD coating shows formation of very fine floes that are separated by fine cracks or larger voids of absent coating. These voids expose the underlying substrate and lead to subsequent adhesive wear (present in other locations of the valve plate, not shown). It is believed that this failure mode is a direct consequence of insufficient substrate hardness for this coating leading to an eggshell effect, which might be improved by modifying the substrate material or heat treatment.

Summarized and categorized, several main failure mechanisms were identified:

- Insufficient shear stress stability due to weakened grain boundaries and/or transformed material
- Insufficient bonding strength of coatings on the substrate resulting in delamination of the coating
- Insufficient ductility of coatings leading to crack formation and subsequent delamination of the coating

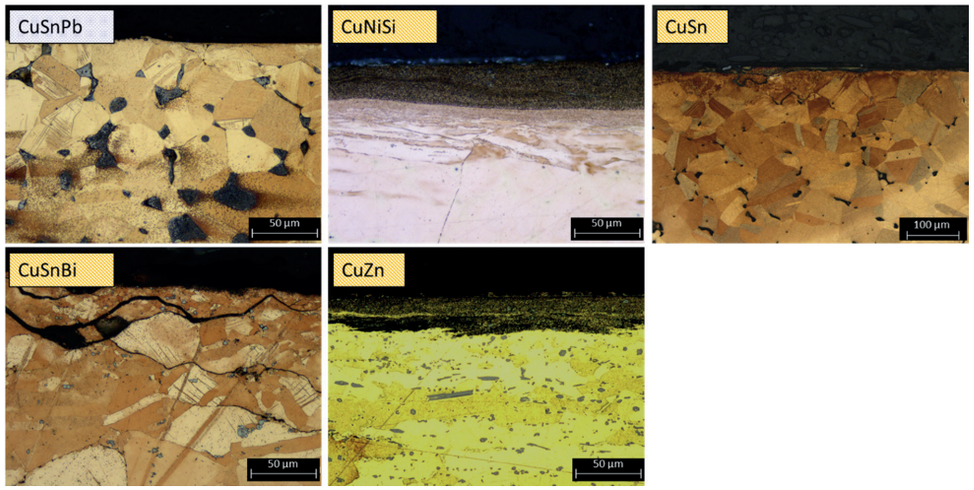

Figure 10: Microstructure of the copper-based tested materials

Comparing these results with the pin-on-disc tribometer results, a significant difference becomes obvious. Even if statements concerning materials-related coefficient of friction will remain identical, the component tests showed a completely different wear performance and durability, e.g. thermally sprayed coatings which have shown excellent performance during the tribometer test, failed in very early load stages of the component test. This can be explained by the higher grade of complexity of the dynamic system and contributing factors like fluid pressure-induced part deflection, tribological interface geometry with resulting break-in behaviour and fully formulated HLP-class fluid usage in comparison with the static system of a tribometer.

5 Summary and Conclusion

One goal of this study was to benchmark commonly available RoHS-compliant bearing materials against the current state-of-the-art leaded-bronze for application in hydrostatic axial piston pumps and motors. In addition to that, indications towards a more systematic approach to optimize that interface by materials choice were needed. Therefore, the tribological performance and durability of leaded-bronze (CuSn10Pb10) on a steel backing has been compared with the behaviour of potential substitutes, namely lead-free copper-based bi-metals and bulk materials, thermally sprayed coatings and PVD coatings, in a pin-on-disc tribometer and a full-sized axial piston pump test rig. For both testing methods, a major focus was on the actual wear mechanism and progression to identify principally influencing (and limiting) factors on durability in hydrostatic components.

The pin-on disc test results are strongly dependent on material properties such as hardness and surface roughness of both contact partners and can successfully be applied to determine basic material properties. During this study, the pin-on-disc test has shown significant principal differences in the progression of the coefficients of friction of different materials, which are explained by sample properties like hardness and surface texture. In the end, however, indications for superior wear performance, like constantly low coefficients and minor wear of wear tracks, were not transferable to component tests. This was explained by the higher grade of complexity of acting factors like fluid pressure-induced part deflection, tribological interface geometry with resulting break-in behaviour and fully formulated HLP-class fluid usage. For future material developments to be used in hydrostatic components, it is therefore almost mandatory to increase the complexity level of tribometers from level three (DIN 50322) to a higher level by adapting component properties like similar interface geometry (i.e. ring-on-ring instead of pin-on-disc to mimic the valve plate / cylinder block interface) and maybe even including the balancing of hydrodynamic and hydrostatic lubrication by adding kidneys into the rings and pressurized lubrication. By doing that, the tribological conditions in such a tribometer would become more similar to the actual conditions in a hydrostatic pump or motor. Then, in the end, the high effort and costs of component tests would be lessened or could even be completely avoided when testing alternative materials for the axial sliding bearing interface to improve durability.

From a wear analysis perspective, the component tests resulted in a new fundamental understanding of critical characteristics that materials must exhibit to achieve sufficient tribological performance and durability in hydrostatic components, including, but not limited to low adhesive wear tendency and low coefficient of friction in mixed lubrication conditions, sufficient bonding strength in the case of coatings and certain fatigue resistance. One big difference to automotive bearings, which explains important additional requirements, is the fact that the tribological interface not only functions as a sealing and lubricating gap but also as a load-carrying element, which results in parts deflection and very high metal-to-metal contact pressures in case of fluid-film break-down. One of these additional requirements was found to be the material's ability to withstand detrimental friction-induced material transformation in high-speed metal-to-metal contact situations, already known from amorphous carbon coatings (DLC), but now also shown for certain copper-based bearing materials. Another key element identified is the material's ductility to withstand high stresses caused by pressure-induced parts deflection and vapour cavitation effects.

All findings together generally, show the difficulty to directly transfer well-established bearing material solutions from automotive applications to hydrostatic pumps and motors. However, with further holistic optimization of all the above-mentioned factors and therefore tailoring of material properties to the demands of axial sliding bearings in hydrostatic pumps and motors, it will become possible to fully substitute and even outperform the leaded bronze in the long term for even the most demanding operating conditions. As an outlook that would finally enable component and machine manufacturers to further optimize machine performance and efficiency while using environmentally acceptable materials at the same time.

Nomenclature

Variable	*Description*	*Unit*
V_w	Wear Volume	[mm^3]
R	Radius of the wear track	[mm]
A_w	Wear area	[mm^2]
PV	PV factor	$[\frac{N}{m \cdot s}]$

References

/1/ Hutching, I., Shipway, P., *Tribology: Friction and Wear of Engineering Materials*, 2nd edition, p.316, 2017.

/2/ Davis, J. R., *Copper and Copper Alloys*, ASM Specialty Handbook, ASM International, Ohio, United States of America, p. 91, 2001.

/3/ Donnet, C., Erdemir, A., *Tribology of Diamond-Like Carbon Films*, Springer, New York, USA, 2008

/4/ Jung,H. -S., Park, H. -H., Pang,S. S., Lee, S.Y., *Thin Solid Films*, 355-356, pp.151-156, 1999

/5/ Paulus, A., *Tribolayer Formation on Bronze CuSn12Ni2 in the Tribological Contact between Cylinder and Control Plate in an Axial Piston Pump with Swashplate Design*, 10th international Fluid Power Conference, 10. IFK, Dresden, Germany, March 8-10, 2016

/6/ Prasad, B.K., *Sliding wear behavior of bronzes under varying material composition, microstructure and test conditions*, Wear 257, pp. 110-123, 2004

/7/ Oksanen, V.T., Jehtovaara, A.J., Kallio, M.H., *Load capacity of lubricated bismuth bronze bimetal bearing under elliptical sliding motion*, Wear, Vol.388-389, pp. 72-80, 2017

/8/ VICTREX® PEEK, Properties Brochure, © Victrex plc March 2016

/9/ Barbezat, G., *Advanced thermal spray technology and coating for lightweight engine blocks for the automotive industry*, Surface and Coatings Technology, Vol. 200, Issues 5-6, pp 1990-1993, 2005

/10/ Totten, G.E., *Handbook of Hydraulic Fluid Technology (Mechanical Engineering)*, Marcel Dekker, Inc., New York, USA, p. 387 , 1999

/11/ Y. G. Yin et al., *Study on Mechanical Properties of Cu-Bi Bearing Materials*, Advanced Materials Research, Vols. 756-759, pp. 89-92, 2013